Efficient Integral Equation Method for the Solution of 3-D Magnetostatic Problems

Wolfgang Hafla, André Buchau, Friedemann Groh, and Wolfgang M. Rucker

Institute for Theory of Electrical Engineering, University of Stuttgart, 70569 Stuttgart, Germany

Nonlinear three-dimensional (3-D) magnetostatic field problems are solved using integral equation methods (IEM). Only the nonlinear material itself has to be discretized. This results in a system of nonlinear equations with a relative small number of unknowns. To keep computational costs low the fully dense system matrix is compressed with the fast multipole method. The accuracy of the applied indirect IEM formulation is improved significantly by the use of a difference field concept and a special treatment of singularities at edges. An improved fixed point solver is used to ensure convergence of the nonlinear problem.

Index Terms—**Equivalent magnetic charges, fast multipole methods, integral equation methods, nonlinear magnetostatics.**

I. Introduction

THE boundary element method (BEM) is very popular for solving linear static field problems. Especially indirect BEM formulations based on equivalent surface charge densities can be supplemented with volume integral equations to handle nonlinear material where equivalent volume charges occur. This generalized treatment is called integral equation method (IEM).

Equivalent charges cannot be calculated directly as in the case of large permeabilities the field strength inside the magnetic material is very low and cancellation errors become significant. To reduce this influence of truncation errors to the solution of the whole problem a difference field concept is applied [1]–[3].

Compared with finite element method (FEM), the advantages of the IEM lie mainly in the minimum number of unknowns, as only regions with nonlinear material have to be meshed with volume elements. Also boundary conditions at infinity are inherently fulfilled. On the other hand the system matrix of an IEM is fully dense.

In the case of volume meshes a compression technique which results in very low memory requirements is required, e.g., the fast multipole method (FMM) [4], [5]. The computational costs and memory requirements are reduced drastically [6].

The error of the solution is significantly influenced by the field near edges or in corners [7]. Therefore, a special treatment at these locations is necessary [8]. The number of iteration steps in the linear and the nonlinear solver influences the computational costs of the solution process. On the one hand, a small number of iterations is desired but on the other hand convergence, especially of the nonlinear solver, must be ensured. Therefore, an improved direct iteration solver is considered.

II. Integral Equation Method

The investigated setup consists of free space, a current-free region Ω_m with surface S and relative permeability μ_r, and a coil region Ω_S within free space that carries a prescribed current density $\boldsymbol{J}$. The resulting field strength can be written as

$$\boldsymbol{H}(\boldsymbol{r}) = \boldsymbol{H^S}(\boldsymbol{r}) + \boldsymbol{H^i}(\boldsymbol{r}) \tag{1}$$

where $\boldsymbol{H^i}$ is the induced magnetic field and $\boldsymbol{H^S}$ is the source field due to free currents $\boldsymbol{J}$ which can be calculated with Biot–Savart's Law. The unknowns of the problem are the sources of $\boldsymbol{H^i}$. It is clear that with this approach $\boldsymbol{H^i}$ is inherently irrotational and, therefore, only the induction's solenoidality $(\operatorname{div}\boldsymbol{B} = 0)$ has to be fulfilled. This approach results in two integral equations which have to be solved simultaneously.

A. Integral Equation From Induction's Solenoidality on S

Applying $\operatorname{div}\boldsymbol{B} = 0$ for points on the surface of Ω_m yields the integral equation [9], [10]

$$\frac{\sigma(\boldsymbol{r})}{2\lambda(\boldsymbol{r})} - \left[\int_A \sigma(\boldsymbol{r}')\partial_{\boldsymbol{n}} G(\boldsymbol{r},\boldsymbol{r}')\mathrm{d}A' + \int_V \rho(\boldsymbol{r}')\partial_{\boldsymbol{n}} G(\boldsymbol{r},\boldsymbol{r}')\mathrm{d}V'\right] = \boldsymbol{n}(\boldsymbol{r})\cdot\boldsymbol{H^S}(\boldsymbol{r}) \tag{2}$$

with free space Green's function G, its normal derivative $\partial_{\boldsymbol{n}} G$, and

$$\lambda(\boldsymbol{r}) = [\mu_r(\boldsymbol{r}) - 1]/[\mu_r(\boldsymbol{r}) + 1] \tag{3}$$

for the unknown equivalent surface and volume charges σ and ρ, respectively. The normal vector $\boldsymbol{n}$ points outwards from Ω_m. As in highly permeable materials that are not penetrated by Ω_S, $\boldsymbol{H}$ is very small and huge cancellation errors occur [11]. To overcome this problem it was proposed [2], [13] to solve the problem in a first step for infinite permeability. In that case, for

$$\boldsymbol{H} = \boldsymbol{H}^i|_{\mu_r\to\infty} + \boldsymbol{H}^s = 0 \tag{4}$$

so volume charges do not occur. Setting $\lambda = 1$ in (2) results in

$$\frac{1}{2}\sigma_\infty(\boldsymbol{r}) + \int_A \sigma_\infty(\boldsymbol{r}')\partial_{\boldsymbol{n}}(\boldsymbol{r},\boldsymbol{r}')\mathrm{d}A' = \boldsymbol{n}(\boldsymbol{r})\cdot\boldsymbol{H^S}(\boldsymbol{r}). \tag{5}$$

Digital Object Identifier 10.1109/TMAG.2005.844342

Once (5) has been solved, it can be used to substitute the right-hand side of (2). This leads with the difference surface charge

$$\delta\sigma = \sigma - \sigma_\infty \tag{6}$$

to the integral equation

$$\frac{\delta\sigma(\boldsymbol{r})}{2} + \lambda(\boldsymbol{r})\left[\int_A \delta\sigma(\boldsymbol{r}')\partial_{\boldsymbol{n}} G(\boldsymbol{r},\boldsymbol{r}')\,\mathrm{d}A' + \int_V \rho(\boldsymbol{r}')\partial_n G(\boldsymbol{r},\boldsymbol{r}')\,\mathrm{d}V'\right] = \sigma_\infty(\boldsymbol{r})[\lambda(\boldsymbol{r})-1]/2. \tag{7}$$

From (4), it follows that

$$\boldsymbol{H^S}(\boldsymbol{r}) = -\boldsymbol{H^i}(\boldsymbol{r})|_{\mu_r\to\infty} = \int_A \sigma_\infty(\boldsymbol{r}')\nabla G(\boldsymbol{r},\boldsymbol{r}')\,\mathrm{d}A' \tag{8}$$

so the induced magnetic field can be computed with

$$\boldsymbol{H}(\boldsymbol{r}) = -\int_V \rho(\boldsymbol{r}')\nabla G(\boldsymbol{r},\boldsymbol{r}')\,\mathrm{d}V' - \int_A \begin{Bmatrix} \delta\sigma(\boldsymbol{r}') \\ [\delta\sigma+\sigma_\infty](\boldsymbol{r}') \end{Bmatrix} \nabla G(\boldsymbol{r},\boldsymbol{r}')\,\mathrm{d}A' + \begin{Bmatrix} 0 \\ H^{\boldsymbol{S}}(\boldsymbol{r}) \end{Bmatrix} \text{ if } \begin{Bmatrix} \boldsymbol{r}\in\Omega_m \\ \boldsymbol{r}\notin\Omega_m \end{Bmatrix}. \tag{9}$$

B. Integral Equation From Induction's Solenoidality in Ω_m

In cases where the permeable material is nonlinear, i.e.,

$$\mu_r(H) = \frac{B(H)}{\mu_0 H} \tag{10}$$

is not constant, solenoidality of induction within Ω_m leads to [11] nonvanishing volume charges

$$\rho(\boldsymbol{r}) + \mu_0 \boldsymbol{H}(\boldsymbol{r})\cdot\nabla\ln\mu_r(\boldsymbol{r}) = 0. \tag{11}$$

For $\boldsymbol{r}\in\Omega_m$, (9) can be substituted into (11) in order to obtain

$$\rho(\boldsymbol{r}) - \int_V \rho(\boldsymbol{r}')\nabla G(\boldsymbol{r},\boldsymbol{r}')\cdot\nabla\ln\mu_r(\boldsymbol{r})\,\mathrm{d}V' - \int_A \delta\sigma(\boldsymbol{r}')\nabla G(\boldsymbol{r},\boldsymbol{r}')\cdot\nabla\ln\mu_r(\boldsymbol{r})\,\mathrm{d}A' = 0. \tag{12}$$

III. Discretization

To achieve high accuracy we decided to apply Galerkin's Method [14] for discretization. We get from (5)

$$[A^\infty]\cdot\{\sigma_\infty\} = \{h^S\} \tag{13}$$

with

$$A_{ij}^\infty = \int_{A_i} M_i(\boldsymbol{r})\left(\frac{M_j(\boldsymbol{r})}{2} + \int_{A_j} M_j(\boldsymbol{r}')\boldsymbol{n}(\boldsymbol{r})\cdot\nabla G(\boldsymbol{r},\boldsymbol{r}')\,\mathrm{d}A'\right) \tag{14}$$

$$h_i^S = \int_{A_i} M_i(\boldsymbol{r})\boldsymbol{H^S}(\boldsymbol{r})\cdot\boldsymbol{n}(\boldsymbol{r})\,\mathrm{d}A \tag{15}$$

where M_i is the sum of all element shape functions associated with node i. The coupled equations (7) and (12) yield

$$\begin{bmatrix} [A^{\sigma\sigma}] & [A^{\sigma\rho}] \\ [A^{\rho\sigma}] & [A^{\rho\rho}] \end{bmatrix} \cdot \begin{Bmatrix} \{\delta\sigma\} \\ \{\rho\} \end{Bmatrix} = \begin{Bmatrix} \{b\} \\ 0 \end{Bmatrix} \tag{16}$$

with

$$A_{ij}^{\sigma\sigma} = \int_{A_i} M_i(\boldsymbol{r})\left(\frac{M_j(\boldsymbol{r})}{2} + \lambda(\boldsymbol{r})\int_{A_j} M_j(\boldsymbol{r}')\partial_n G(\boldsymbol{r},\boldsymbol{r}')\,\mathrm{d}A'\right)\mathrm{d}A \tag{17}$$

$$A_{ij}^{\sigma\rho} = \int_{A_i} M_i(\boldsymbol{r})\lambda_r \int_{V_j} M_j(\boldsymbol{r}')\partial_n G(\boldsymbol{r},\boldsymbol{r}')\,\mathrm{d}V'\,\mathrm{d}A \tag{18}$$

$$A_{ij}^{\rho\sigma} = \int_{V_i} M_i(\boldsymbol{r})\int_{A_j} M_j(\boldsymbol{r}')\nabla G(\boldsymbol{r},\boldsymbol{r}')\cdot\nabla\ln\mu_r(\boldsymbol{r})\,\mathrm{d}A'\,\mathrm{d}V \tag{19}$$

$$A_{ij}^{\rho\rho} = \int_{V_i} M_i(\boldsymbol{r})\left(M_j(\boldsymbol{r}) - \int_{V_j} M_j(\boldsymbol{r}')\nabla G(\boldsymbol{r},\boldsymbol{r}')\cdot\nabla\ln\mu_r(\boldsymbol{r})\,\mathrm{d}V'\right)\mathrm{d}V \tag{20}$$

$$b_i = \frac{1}{2}\sum_j \sigma_{\infty,j}\int_{A_i}[\lambda(\boldsymbol{r})-1]M_i(\boldsymbol{r})M_j(\boldsymbol{r})\,\mathrm{d}A. \tag{21}$$

First, (13) has to be solved. Because only the surface of Ω_m that borders on free space has to be considered, the computational costs are relatively small.

As (16) is, in general, nonlinear it has to be solved iteratively. In every step of the direct iteration procedure (16) is solved for a linear inhomogeneous distribution of μ_r. New values of μ_r have to be calculated for each nonlinear iteration step. Typical $\mu_r(H)$ characteristics have a maximum. If H_m is the field strength where this maximum occurs, new values of iteration step k are obtained by

$$\mu_r^{(k)} = \begin{cases} B\left(H^{(k)}\right)/\left(\mu_0 H^{(k)}\right), & H^{(k)} < H_m \\ \tilde{B}^{(k)}\Big/\left(\mu_0 H\left(\tilde{B}^{(k)}\right)\right), & H^{(k)} \geq H_m \end{cases} \tag{22}$$

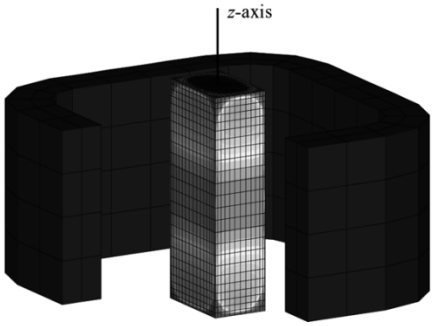

Fig. 1. Steel plate within a coil. On the surface of the steel plate the distribution of the magnetic flux density is displayed. For graphical representation purposes a quarter of the coil is omitted.

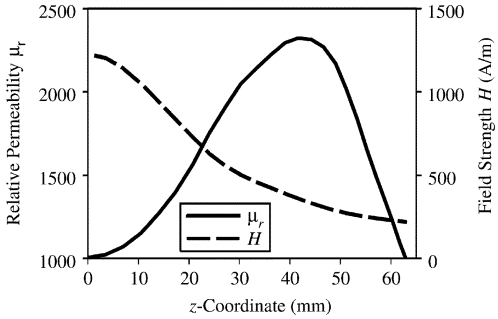

Fig. 2. Magnitude of magnetic field strength and relative permeability at z-axis calculated with the proposed IEM formulation.

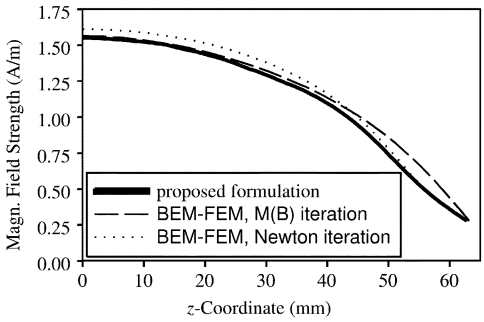

Fig. 3. Magnitude of magnetic flux density at z-axis calculated with the proposed IEM formulation as well as two finite element formulations.

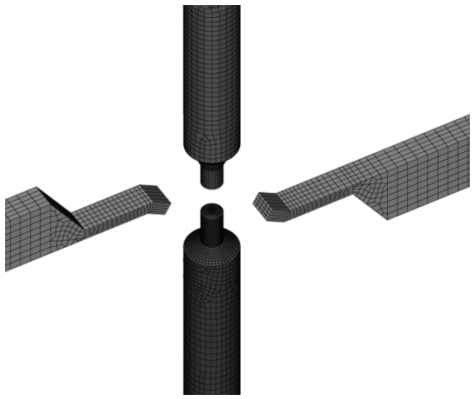

Fig. 4. Investigated arrangement of pole shoes for Magnetic Transmission X-ray Microscopy Project (6812 surface elements, 3130 volume elements, 36 912 unknowns).

with the inverse magnetization characteristic $H(B)$ and $\tilde{B}^{(k)} = \mu_r^{(k-1)} H^{(k)}$. This procedure allows global convergence even if the material is mainly in the steep section of the $B(H)$-characteristic. To accelerate the iteration, super-relaxation with a carefully chosen relaxation parameter is used. Iteration is stopped when the deviations $\mathrm{mean}(\Delta\mu/\mu)$ and $\max(\Delta\mu/\mu)$ are sufficiently small.

Different to the extended boundary element method (EBEM) [11] the whole system matrix in (16) is assembled. Both surface and volume charges are obtained as solution of (16). For each nonlinear iteration step only new relative permeabilities have to be calculated with (22). With EBEM in every nonlinear step estimated values for unknown volume charges are assumed known and put to the right-hand side. Hence, both new volume charges and new relative permeabilities have to be determined for each nonlinear step.

Special treatment is taken when the field strength in (22) is calculated at nodes that lie on edges or corners of S. In that case, it becomes infinite [7]. For the sake of realistic values, edges and corners are numerically rounded off [8].

The FMM has been already successfully applied to the BEM [5]. To use it with IEM, the multipole expansion of volume charges has to be calculated additionally to the one of the surface charges. Also, the different sizes of surface and volume elements have to be considered for the grouping scheme [14].

IV. Numerical Results

We tested the proposed formulation with isoparametric second-order elements. As linear solver GMRES in combination with a Jacobi preconditioner was used. To prevent the iteration procedure to become unstable, relative permeability is interpolated bilinear. As linear field problems already showed excellent accuracy [3] only nonlinear examples are presented. Our calculations were run on a 2-GHz Intel Xeon computer.

A. Steel Cube Within Racetrack Coil

As shown in Fig. 1 a steel plate with dimensions 32 $\times$ 50 $\times$ 126.4 mm is placed in the center of a racetrack coil. Coil dimensions and initial curve are taken from TEAM Workshop Problem 13 [15]. The coil is excited by 22 500 AT. After 19 iterations with super relaxation factor $\omega = 1.1$ and 226 326 seconds the stopping criteria $\mathrm{mean}(\Delta\mu/\mu) < 5\%$ and $\max(\Delta\mu/\mu) < 1\%$ were fulfilled. Memory requirements were reduced by the FMM from 5.16 to 0.95 GByte with 26 315 unknowns (4608 volume and 1728 surface elements).

The magnetic field and relative permeability in Fig. 2 were calculated along the z-axis within the steel plate. The results of our proposed formulation and two different BEM–FEM formulations [16] for the magnetic flux density are depicted in Fig. 3 and show good agreement.

B. Magnetic Transmission X-Ray Microscopy Project

For the MTXM Project at BESSY II [17], the field distribution in the air region between the pole shoes shown in Fig. 4 was investigated.

The flux lines run between the horizontal pole shoes. The influence of the passive vertical pole shoes was to be investigated especially at the sample location which is directly above

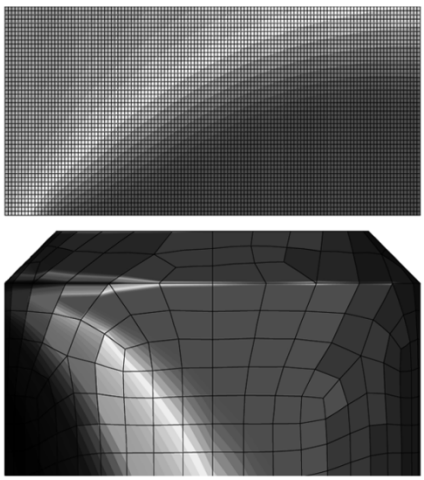

Fig. 5. Magnitude of flux density directly above lower pole shoe.

the lower one. The vertical pole shoes do not saturate, so their relative permeability could be assumed constant, e.g., 1700.

The stopping criterion of mean$(\Delta\mu/\mu) < 2.5\%$ of the nonlinear solver was chosen to obtain accurate results in the interesting region. It was reached after 28 iterations and 406 800 s. As the system matrix was compressed with the FMM only 729 MByte were required to solve the problem. Without the FMM about 10.1 GByte would have been necessary.

Flux density was calculated at the nodes of the very fine evaluation mesh (19101 nodes) shown in Fig. 5. The calculation of the field at all 28 389 evaluation points took only 2 min.

V. Conclusion

Nonlinear magnetostatic field problems have been solved with a new equivalent charge formulation. Uniform treatment of surface and volume charges results in an elegant coupling of integral equations. Nonlinear problems are treated by consecutively solving linear problems. After each nonlinear step only new values of relative permeability have to be calculated. Application of the FMM leads to large reductions of CPU time and especially of memory requirements. Furthermore, all well-known IEM techniques still can be used.

The formulation was tested against BEM-FEM calculations and showed good agreement.

Acknowledgment

This work was supported in part by the Deutsche Forschungsgemeinschaft under Contracts ru 720/3-1 and 720/3-2. The authors would like to thank Prof. Bíró from IGTE at TU Graz and A. Hafla from ISW at the University of Stuttgart for kindly supporting them during the verification process of their software.

References

[1] S. Babic, C. Akyel, and M. Gavrilovic, "Calculation improvement of third-linear magnetostatic field based on fictious magnetic surface charge," *IEEE Trans. Magn.*, vol. 36, no. 5, pp. 3125–3127, Sep. 2000.

[2] D. Kim, I. Park, M. Park, and H. Lee, "3-D magnetostatic field calculation by a single layer boundary integral equation method using a difference field concept," *IEEE Trans. Magn.*, vol. 36, no. 5, pp. 3134–3136, Sep. 2000.

[3] W. Hafla, F. Groh, A. Buchau, and W. M. Rucker, "Magnetostatic field computations by a integral equation method using a difference field concept and the fast multipole method," in *Proc. 10th IGTE Symp. Numerical Field Calculation in Electrical Engineering*, 2002, pp. 262–266.

[4] L. Greengard and V. Rokhlin, *The Rapid Evaluation of Potential Fields in Three Dimensions*. ser. Lecture Notes in Mathematics 1360, C. Anderson and C. Greengard, Eds. Berlin, Germany: Springer-Verlag, 1987, pp. 121–141.

[5] A. Buchau, W. Hafla, and W. M. Rucker, "Fast and efficient 3-D boundary element method for closed domains," in *Proc. Symp. Reports 6th Int. Symp. Electric and Magnetic Fields*, Aachen, Germany, 2003, pp. 211–214.

[6] A. Buchau, W. M. Rucker, O. Rain, V. Rischmüller, S. Kurz, and S. Rjasanow, "Comparison between different approaches for fast and efficient 3-D BEM computations," *IEEE Trans. Magn.*, vol. 39, no. 3, pp. 1107–1110, Jun. 2003.

[7] S. Peaiyoung and S. J. Salon, "Some technical aspects of implementing boundary element equations," *IEEE Trans. Magn.*, vol. 25, no. 4, pp. 2998–3000, Jul. 1989.

[8] F. Groh, W. Hafla, A. Buchau, and W. M. Rucker, "Field strength computation at edges in nonlinear magnetostatics," in *Conf. Proc. XI Int. Symp. Electromagnetic Fields in Electrical Engineering*, 2003, pp. 243–246.

[9] J. H. McWhirter, J. J. Oravec, and R. W. Haak, "Computation of magnetostatic fields in three-dimensions based on Fredholm integral equations," *IEEE Trans. Magn.*, vol. MAG-18, no. 2, pp. 1088–1091, Mar. 1982.

[10] D. A. Lindholm, "Notes on boundary integral equations for three-dimensional magnetostatics," *IEEE Trans. Magn.*, vol. MAG-16, no. 6, pp. 1409–1412, Nov. 1980.

[11] B. Krstajić, Z. Andelić, S. Milojković, and S. Babiæ, "Non-linear 3-D magnetostatic field calculation by the integral equation method with surface and volume magnetic charges," *IEEE Trans. Magn.*, vol. 28, no. 2, pp. 1088–1091, Mar. 1992.

[12] C. Magele, H. Stögner, and K. Preis, "Comparison of different finite element formulations for 3-D magnetostatic problems," *IEEE Trans. Magn.*, vol. 24, no. 1, pp. 31–34, Jan. 1988.

[13] I. D. Mayergoyz, M. V. K. Chari, and J. D'Angelo, "A new scalar potential formulation for three-dimensional magnetostatic problems," *IEEE Trans. Magn.*, vol. MAG-23, no. 6, pp. 3889–3894, Nov. 1987.

[14] A. Buchau, W. Hafla, F. Groh, and W. M. Rucker, "Grouping schemes and meshing strategies for the fast multipole method," in *COMPEL*, vol. 22, 2003, pp. 495–507.

[15] T. Nakata, N. Takahashi, K. Fujiwara, P. Olszewski, K. Muramatsu, T. Imai, and Y. Shiraki, "Numerical analysis and experiments of 3-D nonlinear magnetostatic model," in *Proc. Int. Symp. TEAM Workshop, Supplement A*, Okayama, Japan, 1990, pp. 308–310.

[16] S. Kurz, J. Fetzer, and G. Lehner, "A novel iterative algorithm for the nonlinear BEM-FEM coupling method," *IEEE Trans. Magn.*, vol. 33, no. 2, pp. 1772–1775, Mar. 1997.

[17] T. Eimüller, "Magnetic imaging of nanostructured systems with transmission X-Ray microscopy," Ph.D. dissertation, Universität Würzburg, Würzburg, Germany.

Manuscript received June 7, 2004.